

# Importance of three-body forces for nucleus-nucleus scattering

T. Furumoto\*

*Department of Physics, Osaka City University, Osaka 558-8585, Japan*

Y. Sakuragi†

*Department of Physics, Osaka City University, Osaka 558-8585, Japan,  
and RIKEN Nishina Center, RIKEN, Wako, Saitama 351-0198, Japan*

Y. Yamamoto‡

*Physics Section, Tsuru University, Tsuru, Yamanashi 402-8555, Japan*

(Dated: February 13, 2009)

The effect of three-body force (TBF) is studied in nucleus-nucleus elastic scattering on the basis of Brueckner theory for nucleon-nucleon ( $NN$ ) effective interaction (complex G-matrix) in nuclear matter. A new G-matrix called CEG07 proposed recently by the present authors includes the TBF effect and reproduces a realistic saturation curve in nuclear matter, and is shown to well reproduce proton-nucleus elastic scattering. The microscopic optical potential for  $^{16}\text{O} + ^{16}\text{O}$  system is obtained by folding the G-matrix with nucleon density distributions in colliding nuclei. The observed cross sections for  $^{16}\text{O} + ^{16}\text{O}$  elastic scattering at  $E/A = 70$  MeV are well reproduced up to the most backward scattering angles only when the TBF effect is included. The CEG07 G-matrix is also tested in the elastic scattering of  $^{16}\text{O}$  by the  $^{12}\text{C}$  target at  $E/A = 93.9$  MeV, and in the elastic scattering of  $^{12}\text{C}$  by  $^{12}\text{C}$  target at  $E/A = 135$  MeV with a great success.

PACS numbers: 21.30.-x, 21.65.-f, 24.10.Ht, 25.70.Bc

## I. INTRODUCTION

The role of nuclear three-body force (TBF) in complex nuclear systems is one of the key issue not only in nuclear physics but also in nuclear astrophysics relevant to high-density nuclear matter in neutron stars and supernova explosions. It is well known that the empirical saturation point of nuclear matter (the binding energy per nucleon  $E/A \approx 16$  MeV at a saturation density  $\rho_0 \approx 0.17 \text{ fm}^{-3}$ ) cannot be reproduced by using only two-body  $NN$  interactions [1]. In order to obtain the reasonable saturation curve, it is indispensable to take into account the additional contributions of the TBF which contains the two parts of the three-body attraction (TBA) and the three-body repulsion (TBR). It is important here that the saturation curve in high-density region is strongly pushed up by the TBR contribution and the nuclear-matter incompressibility becomes large as a result [2–5]. This effect is intimately related to our problem. In Ref. [6], we reported for the first time a clear evidence of important role of TBF (especially TBR) in nucleus-nucleus elastic scattering in the case of  $^{16}\text{O} + ^{16}\text{O}$  system at  $E/A = 70$  MeV. In this paper, we also show a clear evidence of decisive role of TBF in other systems.

It is a longstanding and fundamental subject to understand nucleon-nucleus ( $NA$ ) and nucleus-nucleus ( $AA$ ) interactions microscopically starting from basic nucleon-

nucleon ( $NN$ ) interaction. In order to solve a complicated many-body problem in nuclear reactions, one needs to rely upon some realistic approach based on reasonable approximations. One of the promising approaches would be to derive the  $NA$  and  $AA$  folding potentials on the basis of the lowest-order Brueckner theory. Here, the  $NN$  G-matrix interactions are obtained in infinite nuclear matter, and folded into  $NA$  and  $AA$  density distributions with the local-density approximation (LDA). The G-matrix equation is solved for a  $NN$  pair in medium, one of which corresponds to an inside nucleon, under the scattering boundary condition. The obtained G-matrix interaction is composed of real and imaginary parts, being dependent on the incident energy and the nuclear-matter density. As noted here, the G-matrix is considered to be an effective  $NN$  interaction in folding procedures, where short-range singularities in a free-space  $NN$  interaction are smoothed out.

The folding-model study with the use of complex G-matrix interactions for  $NA$  system has a long history. Various G-matrix interactions starting from different kind of free-space  $NN$  interactions were proposed and applied to the analyses of proton-nucleus elastic scattering with more or less successful results. However, all the G-matrix proposed so far were derived only from two-body force and the effect of TBF was not included nor discussed. This is partly because the TBF contributions in lower densities than  $\rho_0$  have been considered to be not large enough to affect  $NA$  scattering observables. Here, the local density felt by the incident nucleon inside the target nucleus does not exceed  $\rho_0$  even at deep inside the nucleus.

Recently, the present authors have proposed a new G-

---

\*Electronic address: furumoto@ocunp.hep.osaka-cu.ac.jp

†Electronic address: sakuragi@ocunp.hep.osaka-cu.ac.jp

‡Electronic address: yamamoto@tsuru.ac.jp

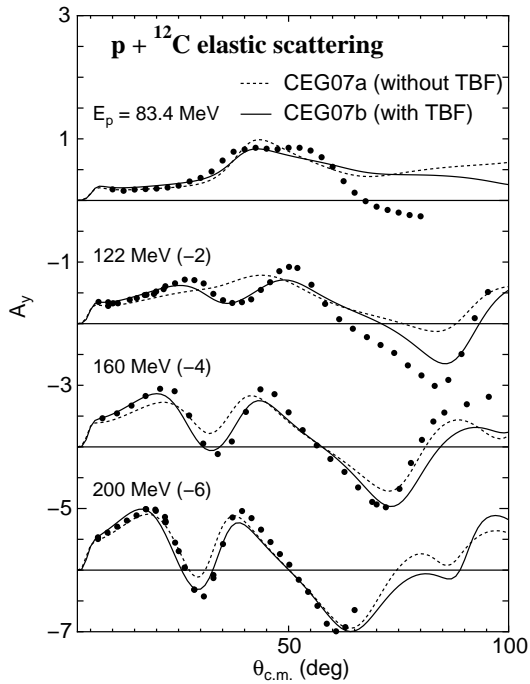


FIG. 1: Analyzing powers for proton elastic scattering by  $^{12}\text{C}$  target at  $E_p = 65 \sim 200$  MeV, which are compared with the folding model calculations with the two types of complex G-matrix interactions. The dotted and solid curves are the results with CEG07a and CEG07b, respectively. The experimental data are taken from Ref. [11–13]

matrix interaction *CEG07* [7] derived from the extended soft-core (ESC) model [8, 9]. The ESC model is designed so as to give a consistent description of interactions not only for *NN* system but also for nucleon-hyperon and hyperon-hyperon systems, where the TBR effect is taken into account effectively by changing vector-meson masses in a density-dependent way. On the other hand, the TBA part is typically due to two-pion exchange with excitation of an intermediate  $\Delta$ -resonance, that is the Fujita-Miyazawa diagram, which gives an important contribution at low densities. In Ref. [7], the TBA effect was included as an effective two-body interaction according to the formalism of Ref. [10] and added to the G-matrix obtained from the two-body interaction. Although the saturation curve of nuclear matter can be produced reasonably as combined contributions of TBA and TBR, it is decisively important in our results that the TBR contribution becomes more and more remarkable as the density increases. Following Ref. [7], we call the G-matrix interaction derived from the ESC part only as CEG07a and the version including further the effect of TBF (both the TBA and TBR components) as CEG07b. The CEG07 models were first applied to the analysis of proton-nucleus elastic scattering over the wide range of incident energy and target nucleus with a remarkable success [7]. Although the inclusion of TBF effect, in general, gave rise to only minor change of *pA* elastic-scattering

cross sections as expected from the above discussion, it was demonstrated that the inclusion of TBR effect clearly improved the fit to forward-angle analyzing power data in some energy region as shown in Fig. 1.

In the case of *AA* scattering system, the local density in the projectile-target overlap region,  $\rho_1 + \rho_2$ , may exceed the normal density of nuclear matter  $\rho_0$  and could reach about twice this value as mentioned later. The TBR contributions are remarkably large in such high-density regions and, hence, one may expect a clear evidence of TBR effect through the calculated folding-model potential and the resultant elastic-scattering observables. The importance of consistent description of nuclear saturation property and elastic scattering of *AA* systems was first pointed out by Khoa *et al.* [14, 15] on the basis of folding-model analyses. They used density-dependent effective *NN* interactions such as those called DDM3Y, BDM3Y and CDM3Y obtained from a density-independent effective interaction M3Y [16] by multiplying various kind of phenomenological density-dependent factors by hand, the parameters of which were chosen so as to represent various types of saturation curves in nuclear matter. The real part of *AA* potential was calculated by the folding of these interactions with nucleon densities of *AA* system, while the imaginary part was treated in a completely phenomenological way because M3Y was composed of real part only. They showed the importance of using an effective interaction to be chosen to reproduce the realistic saturation curve in nuclear matter for the proper description of elastic scattering of *AA* systems. However, their purely phenomenological density-dependent factor had no explicit nor logical relation to the TBF in nuclear medium.

## II. FORMALISM

We construct the nucleus-nucleus optical model potential (OMP) based on the double-folding model (DFM) with the use of complex G-matrix interaction CEG07. The microscopic nucleus-nucleus potential can be written as a Hartree-Fock type potential;

$$U_{\text{DF}} = \sum_{i \in A_1, j \in A_2} [\langle ij | v_{\text{D}} | ij \rangle + \langle ij | v_{\text{EX}} | ji \rangle] \quad (1)$$

$$= U_{\text{D}} + U_{\text{EX}}, \quad (2)$$

where  $v_{\text{D}}$  and  $v_{\text{EX}}$  are the direct and exchange parts of complex G-matrix interaction. The exchange part is a nonlocal potential in general. However, by the plane wave representation for the *NN* relative motion [17, 18], the exchange part can be localized. The direct and exchange parts of the localized potential are then written in the standard form of DFM potential as

$$U_{\text{D}}(R) = \int \rho_1(\mathbf{r}_1) \rho_2(\mathbf{r}_2) v_{\text{D}}(s; \rho, E/A) d\mathbf{r}_1 d\mathbf{r}_2, \quad (3)$$

where  $\mathbf{s} = \mathbf{r}_2 - \mathbf{r}_1 + \mathbf{R}$ , and

$$U_{\text{EX}}(R) = \int \rho_1(\mathbf{r}_1, \mathbf{r}_1 + \mathbf{s}) \rho_2(\mathbf{r}_2, \mathbf{r}_2 - \mathbf{s}) v_{\text{EX}}(s; \rho, E/A) \times \exp\left[\frac{i\mathbf{k}(R) \cdot \mathbf{s}}{M}\right] d\mathbf{r}_1 d\mathbf{r}_2. \quad (4)$$

Here,  $\mathbf{k}(R)$  is the local momentum for nucleus-nucleus relative motion defined by

$$k^2(R) = \frac{2mM}{\hbar^2} [E_{\text{c.m.}} - \text{Re}U_{\text{DF}}(R) - V_{\text{coul}}(R)], \quad (5)$$

where,  $M = A_1 A_2 / (A_1 + A_2)$ ,  $E_{\text{c.m.}}$  is the center-of-mass energy,  $E/A$  is the incident energy per nucleon,  $m$  is the nucleon mass and  $V_{\text{coul}}$  is the Coulomb potential.  $A_1$  and  $A_2$  are mass number of projectile and target, respectively. The exchange part is calculated self-consistently based on the method of local energy approximation through Eq. (5) in the same manner as in Ref. [19]. The detail methods of calculation for  $U_{\text{D}}$  (direct part) and  $U_{\text{EX}}$  (exchange part) are the same as those given in Ref. [20] and [14], respectively.

In the calculation, we employ the so-called frozen density approximation (FDA) for evaluating the local density, in which the density-dependent  $NN$  interaction feels the local density defined as the sum of densities of colliding nuclei evaluated at the middle-point of the interacting nucleon pair;

$$\rho = \rho_1 + \rho_2. \quad (6)$$

The FDA has also widely been used in the standard DFM calculations [14, 15, 21, 22]. The validity of FDA is understood qualitatively by considering that the colliding nuclei can overlap into each other without the disturbance due to the Pauli principle in such a high energy as  $E/A = 70 \sim 135$  MeV. Then, the G-matrix interaction in high-density region over normal density, including the strong TBR, contributes to the folding potential.

Other prescriptions for defining the local density than FDA were also tested and discussed in Refs. [23–25], in which the local density was defined by a kind of average, either geometric average or arithmetic one, of the densities of colliding nuclei (the average-density approximation (ADA)). This prescription largely underestimates the medium effect which leads to too deep folding potentials and one inevitably needs to introduce reduction factors for the calculated folding potential both in the real and imaginary parts to reproduce elastic-scattering cross sections [23–25]. In fact, in all the present cases, we have confirmed that the ADA prescription leads to a poor fitting to the data in comparison with the FDA prescription unless introducing substantial reduction of the calculated folding potential strength.

### III. RESULT

Next, we apply the CEG07 G-matrix interactions to nucleus-nucleus ( $AA$ ) systems through the double-folding

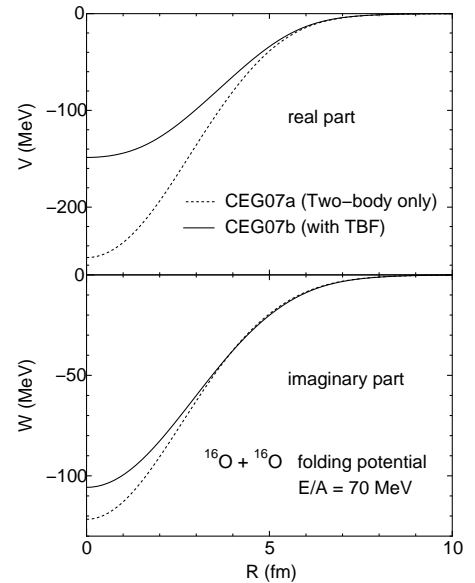


FIG. 2: The real and imaginary part of FMP. The dotted and solid curves are the results with CEG07a and CEG07b, respectively.

model (DFM). Since, the imaginary part of optical potential for  $AA$  systems represents all excurrent flux escaping from elastic scattering channel through all the possible open reaction channels, it would be difficult to completely simulate those flux loss by the imaginary part of G-matrix interaction evaluated in infinite nuclear matter. So, we introduce a renormalization factor  $N_{\text{W}}$  for the imaginary part of folding model potential (FMP) and define the present microscopic optical potential with the CEG07 interaction as

$$U_{\text{DF}}(R) = V_{\text{C}}(R) + iN_{\text{W}}W_{\text{C}}(R). \quad (7)$$

Here,  $V_{\text{C}}$  and  $W_{\text{C}}$  denote the real and imaginary parts of original DFM potential derived from the G-matrix. We adjust the renormalization factor so as to attain optimum fits to the experimental data for elastic scattering cross sections because of the lack of the experimental data for total reaction cross section in most  $AA$  systems.

First, we analyze the elastic scattering of  $^{16}\text{O} + ^{16}\text{O}$  system [6] as a benchmark system for testing the interaction model, and then, we also analyze the  $^{16}\text{O}$  scattering by  $^{12}\text{C}$  target nuclei as well as the  $^{12}\text{C} + ^{12}\text{C}$  scattering. We adopt a nucleon density of  $^{16}\text{O}$  calculated from the internal wave functions generated by the orthogonal condition model (OCM) by S. Okabe [26] based on the microscopic  $\alpha + ^{12}\text{C}$  cluster picture. For  $^{12}\text{C}$ , we use the nucleon density obtained from the  $3\alpha$ -RGM calculation by Kamimura [27].

Figure 2 shows the real (upper panel) and imaginary (lower panel) parts of the calculated FMP for  $^{16}\text{O} + ^{16}\text{O}$  elastic scattering at  $E/A = 70$  MeV with the two types of complex G-matrix interactions. The effect of TBF is clearly seen in the real part of FMP over the whole range

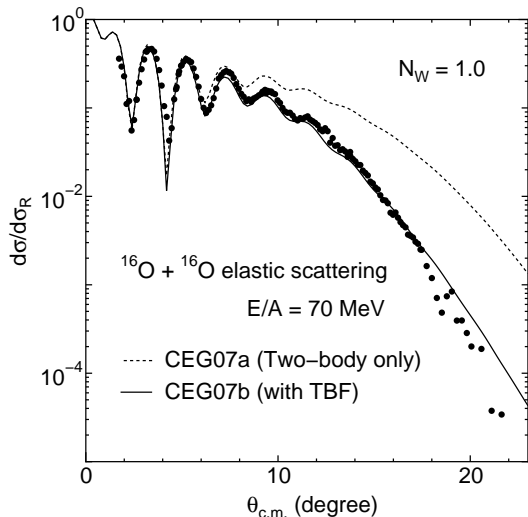


FIG. 3: Differential cross sections for  $^{16}\text{O} + ^{16}\text{O}$  elastic scattering at  $E/A = 70$  MeV, which are compared with the folding model calculations with the two types of complex G-matrix interactions. The meaning of the curves are the same as in Fig. 2. The experimental data are taken from Ref. [28].

of internuclear distance, while the effect on the imaginary part is rather small except at short distances below 3 fm.

We then calculate the  $^{16}\text{O} + ^{16}\text{O}$  elastic scattering cross sections at  $E/A = 70$  MeV with the use of two types of FMPs shown in Fig. 2. In the standard DFMA analyses of elastic scattering, it is often the case that the real part of calculated FMP is multiplied by the renormalization factor while a completely phenomenological imaginary potential is introduced, and its parameters together with the renormalization factor for the real FMP are determined so as to optimize the fit to the experimental data. In the present DFMA, however, the calculated FMP itself is already complex because of the use of complex G-matrix and, hence, no artificial imaginary potential need to be introduced.

The results [6] are shown in Fig. 3. The solid and dotted curves are the results with the use of FMP obtained from CEG07b (with TBF) and CEG07a (without TBF), respectively. The solid curve with the TBF effect well reproduces the experimental data up to backward angles, while the dotted curve with CEG07a (without the TBF effect) overshoots the experimental data at middle and backward angles indicating too deep strength of the real part of FMP. We found that no reasonable fit to the data was obtained by FMP with CEG07a no matter how the imaginary part of FMP is renormalized. When some enhancement factor is multiplied on the imaginary part so as to correct the deviation in the large-angle region, the diffraction pattern in the forward angle region cannot be reproduced as shown in Fig. 4. The large difference between the solid and dotted curves clearly shows an evidence of decisive role of TBF on the elastic scattering of  $^{16}\text{O} + ^{16}\text{O}$  system.

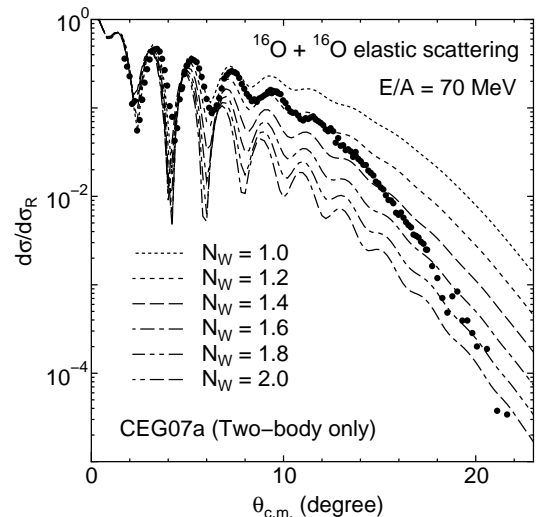


FIG. 4: Same as Fig. 3 but for the results of CEG07a (without TBF) with various renormalization factor for imaginary part.

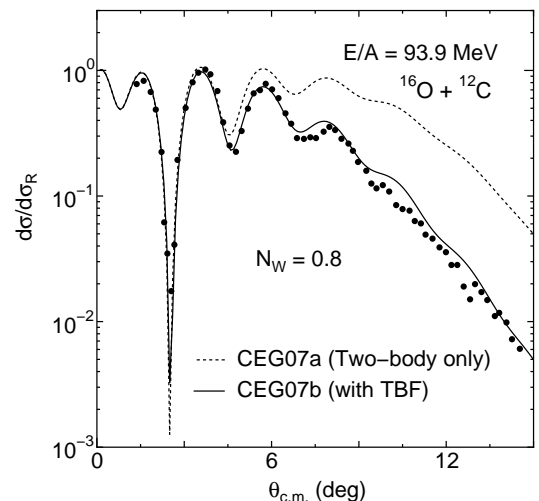


FIG. 5: Same as Fig. 3 but for the  $^{16}\text{O} + ^{12}\text{C}$  system at  $E/A = 93.9$  MeV. The experimental data are taken from Ref. [29].

Figures 5 and 6 show the elastic-scattering cross sections for  $^{16}\text{O} + ^{12}\text{C}$  system at  $E/A = 93.9$  MeV and  $^{12}\text{C} + ^{12}\text{C}$  system at  $E/A = 135$  MeV, respectively. The dotted and solid curves are the results with CEG07a and CEG07b, respectively. CEG07b well reproduces the elastic cross sections up to backward angles with  $N_W = 0.8$  and 0.7. The effect of TBF is clearly seen in cross sections as in the case of  $^{16}\text{O} + ^{16}\text{O}$  scattering seen in Fig. 3. No reasonable fit to the data is obtained by the FMP calculation with CEG07a (without TBF effect), no matter how we change the value of  $N_W$ , which is also the same as in the case of  $^{16}\text{O}$  target shown in Fig. 4.

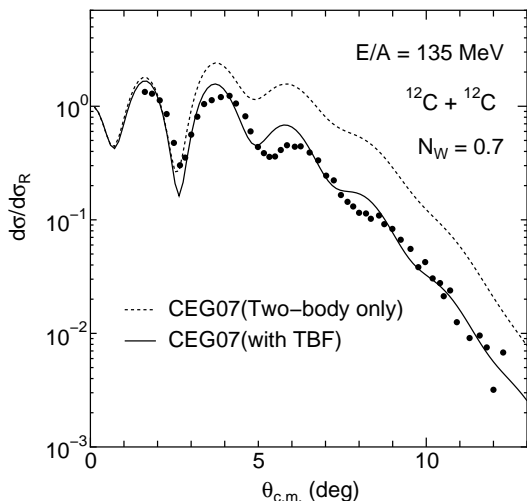


FIG. 6: Same as Fig. 3 but for the  $^{12}\text{C} + ^{12}\text{C}$  system at  $E/A = 135$  MeV. The experimental data are taken from Ref. [30].

#### IV. SUMMARY AND CONCLUSIONS

In summary, we have calculated the differential cross sections for  $^{16}\text{O} + ^{16}\text{O}$ ,  $^{16}\text{O} + ^{12}\text{C}$  and  $^{12}\text{C} + ^{12}\text{C}$  elastic scattering at  $E/A = 70 \sim 135$  MeV with use of the microscopic double folding model given by the two types

of complex G-matrix interactions CEG07a and CEG07b, where the former is derived from the ESC NN interaction model and the latter includes the effect of TBF (TBA+TBR) additionally. Both interactions give rise to the reasonable  $NA$  potentials through the single folding procedures.

The effect of TBF is seen clearly in the inner real part of FMP, where the potential is pushed up remarkably by the TBR contribution in high density region owing to the FDA prescription. Then, the DFM with CEG07b including the TBR effect can reproduce nicely the experimental differential cross sections of all systems. On the other hand, the DFM with CEG07a derived from the two-body interaction only leads to the sizable deviation from the data. Thus, we can conclude that the strong TBR effect in high density region appears clearly in some scattering system of two complex nuclei as well as in nuclear-saturation and astrophysical problems.

#### V. ACKNOWLEDGMENTS

The authors acknowledge Professor Dao T. Khoa for providing with the numeral data of the  $^{16}\text{O} + ^{16}\text{O}$  experimental cross sections. One of the authors (T.F.) is supported by the Japan Society for the Promotion of Science for Young Scientists.

- 
- [1] F. Coester, S. Cohen, B. D. Day, and C. M. Vincent, *Phys. Rev. C* **1**, 769 (1970).
  - [2] I. E. Lagaris and V. R. Pandharipande, *Nucl. Phys.* **A359**, 349 (1981).
  - [3] R. B. Wiringa, V. Fiks, and A. Fabrocini, *Phys. Rev. C* **38**, 1010 (1988).
  - [4] M. Baldo, I. Bombaci, and G. F. Burgio, *Astron. Astrophys.* **328**, 274 (1997).
  - [5] A. Lejeune, U. Lombardo, and W. Zuo, *Phys. Lett.* **B477**, 45 (2000).
  - [6] T. Furumoto, Y. Sakuragi, and Y. Yamamoto, *Phys. Rev. C* **79**, 011601 (2009).
  - [7] T. Furumoto, Y. Sakuragi, and Y. Yamamoto, *Phys. Rev. C* **78**, 044610 (2008).
  - [8] T. A. Rijken, *Phys. Rev. C* **73**, 044007 (2006).
  - [9] T. A. Rijken and Y. Yamamoto, *Phys. Rev. C* **73**, 044008 (2006).
  - [10] T. Kasahara, Y. Akaishi, and H. Tanaka, *Prog. Theor. Phys. Suppl.* **56**, 96 (1974).
  - [11] H. S. M. Ieiri, M. Nakamura, H. Sakamoto, H. Ogawa, M. Yosoi, T. Ichihara, N. Isshiki, Y. Takeuchi, H. Togawa, T. Tsutsumi, et al., *Nucl. Instrum. Methods Phys. Res. A* **257**, 253 (1987).
  - [12] H. O. Meyer, P. Schwandt, W. W. Jacobs, and J. R. Hall, *Phys. Rev. C* **27**, 459 (1983).
  - [13] J. R. Comfort, G. L. Moake, C. C. Foster, P. Schwandt, and W. G. Love, *Phys. Rev. C* **26**, 1800 (1982).
  - [14] D. T. Khoa, W. von Oertzen, and H. G. Bohlen, *Phys. Rev. C* **49**, 1652 (1994).
  - [15] D. T. Khoa, G. R. Satchler, and W. von Oertzen, *Phys. Rev. C* **56**, 954 (1997).
  - [16] G. Bertsch, J. Borysowicz, H. McManaus, and W. G. Love, *Nucl. Phys.* **A284**, 399 (1977).
  - [17] B. Sinha, *Phys. Rep.* **20**, 1 (1975).
  - [18] B. Sinha and S. A. Moszkowski, *Phys. Lett.* **B81**, 289 (1979).
  - [19] J. W. Negele and D. M. Vautherin, *Phys. Rev. C* **5**, 1472 (1972).
  - [20] S. Nagata, M. Kamimura, and N. Yamaguchi, *Prog. Theor. Phys.* **73**, 512 (1985).
  - [21] G. R. Satchler and W. G. Love, *Phys. Rep.* **55**, 184 (1979).
  - [22] M. Katsuma, Y. Sakuragi, S. Okabe, and Y. Kondo, *Prog. Theor. Phys.* **107**, 377 (2002).
  - [23] T. Furumoto and Y. Sakuragi, *Phys. Rev. C* **74**, 034606 (2006).
  - [24] F. Carstoiu and M. Lassau, *Nucl. Phys.* **A597**, 269 (1996).
  - [25] F. Duggan, M. Lassaut, F. Michel, and N. V. Mau, *Nucl. Phys.* **A355**, 141 (1981).
  - [26] S. Okabe, private communication (unpublished).
  - [27] M. Kamimura, *Nucl. Phys.* **A351**, 456 (1981).
  - [28] F. Nuoffer, G. Bartnitzky, H. Clement, A. Blazevic, H. G. Bohlen, B. Gebauer, W. von Oertzen, M. Wilpert, T. Wilpert, A. Lepine-Szily, et al., *Nuovo Cimento A* **111**, 971 (1998).
  - [29] P. Roussel-Chomaz, N. Alamanos, F. Auger, J. Barrette, B. Berthier, B. Fernandez, and L. Papineau, *Nucl. Phys.*

**A477**, 345 (1988).  
[30] T. Ichimura, T. Niizeki, H. Okamura, H. Ohnuma,  
H. Sakai, Y. Fuchi, K. Hatanaka, M. Hosaka, S. Ishida,

K. Kato, et al., Nucl. Phys. **A569**, 287 (1994).